Suppression and Enhancement of Impurity Scattering in a Bose-Einstein Condensate

A. P. Chikkatur, A. Görlitz, D. M. Stamper-Kurn,* S. Inouye, S. Gupta, and W. Ketterle
Department of Physics and Research Laboratory of Electronics, Massachusetts Institute of Technology, Cambridge, Massachusetts 02139
(Received 23 March 2000)

Impurity atoms propagating at variable velocities through a trapped Bose-Einstein condensate were produced using a stimulated Raman transition. The redistribution of momentum by collisions between the impurity atoms and the stationary condensate was observed in a time-of-flight analysis. The collisional cross section was dramatically reduced when the impurity velocity was reduced below the condensate speed of sound, in agreement with the Landau criterion for superfluidity. For large numbers of impurity atoms, we observed an enhancement of atomic collisions due to bosonic stimulation. This enhancement is analogous to optical super-radiance.

PACS numbers: 03.75.Fi, 34.50.–s, 67.90.+z

One manifestation of superfluidity is that objects traveling below a critical velocity v_L through a superfluid propagate without dissipation. Landau [1] used simple kinematic arguments to derive an expression for the critical velocity $v_L = \min[E(p)/p]$, where $E(p)$ is the energy of an elementary excitation with momentum p.

When superfluid ^{4}He was forced through capillaries, adsorbed films, and tightly packed powders [2], the onset of dissipation was found at velocities much lower than the Landau critical velocity due to turbulence and vortex formation in the superfluid. The Landau critical velocity can usually be observed only by moving *microscopic* particles through the superfluid which do not create a macroscopic flow pattern. Studies of superfluidity with microscopic objects were pursued in liquid ^{4}He by dragging negative ions through pressurized ^{4}He [3], and by scattering ^{3}He atoms off superfluid ^{4}He droplets [4].

Atomic Bose-Einstein condensates are superfluid gases and show phenomena analogous to superfluid liquids, albeit at 8 orders of magnitude lower density. For a homogeneous gaseous Bose-Einstein condensate, the Bogoliubov spectrum indicates a Landau critical velocity equal to the speed of sound $v_L = c \equiv \sqrt{\mu/M}$, where μ is the chemical potential and M is the mass of condensate atoms. The first evidence for a critical velocity in a Bose condensate was obtained by stirring the condensate with a *macroscopic* object (a laser beam) [5]. The observed critical velocity was much lower than the speed of sound. Recent studies of superfluidity have revealed quantized vortices [6,7] and a nonclassical moment of inertia [8].

In this Letter, we report on a study of the motion of *microscopic* impurities through a gaseous Bose-Einstein condensate. The impurity atoms were created using a stimulated Raman process which transferred a small fraction of the condensate atoms into an untrapped hyperfine state with well-defined initial velocity. As these impurities traversed the condensate, they dissipated energy by colliding with the stationary condensate, which resulted in a redistribution of momenta of the impurities. As the impurity velocity was reduced below the speed of sound, we observed a dramatic reduction in the probability of collisions, which is evidence for superfluidity in Bose-Einstein condensates.

Our experiments were performed on Bose-Einstein condensates of sodium atoms in the $|F = 1, m_F = -1\rangle$ hyperfine ground state. Condensates of $\sim 10^7$ atoms were created using laser and evaporative cooling and stored in a cylindrically symmetric magnetic trap [9] with an axial trapping frequency of 16 Hz. The density of the condensate was varied by adiabatically changing the radial trapping frequency between 165 and 33 Hz. Hence, the peak speed of sound ranged between 1.1 and 0.55 cm/s.

Impurity atoms were created using a Raman transition, in which the condensate was exposed to a pair of laser beams. The laser beams had orthogonal linear polarizations, thus driving a Raman transition from the trapped $|F = 1, m_F = -1\rangle$ state to the untrapped $|F = 1, m_F = 0\rangle$ hyperfine ground state [10]. The beams passed through two acousto-optic modulators operating with a frequency difference $\omega = \omega_{\mathrm{Zm}} + \hbar q^2/(2M)$, where $\hbar\omega_{\mathrm{Zm}}$ is the Zeeman splitting between the $|m_F = -1\rangle$ and $|m_F = 0\rangle$ states in the offset field of the magnetic trap. The momentum transfer from the light field to the $m_F = 0$ atoms is $\hbar q = 2\hbar k \sin\theta/2$, where k is the light wave vector and θ is the angle between the two laser beams. The Raman light fields were typically pulsed on for about 10 μs at an intensity of several mW/cm^2. The fraction of transferred atoms was varied by changing the light intensity.

Collisions between the impurities and the condensate were analyzed by time-of-flight absorption imaging. For this, the magnetic trap was suddenly switched off 4 ms after the Raman pulse, by which time the impurity atoms had fully traversed the condensate. After an additional 5 ms, a magnetic field gradient was pulsed on for 30 ms, spatially separating the $m_F = 0$ atoms from the condensate. After a total time of flight of typically 60 ms, all atoms were optically pumped into the $|F = 2, m_F = 2\rangle$ state and resonantly imaged on the cycling transition.

Collisions at ultracold temperatures are in the s-wave regime. The products of such collisions between free

particles are evenly distributed [11] in momentum space over a spherical shell around the center-of-mass momentum of the collision partners. A time-of-flight picture records the momentum distribution of the released cloud. Thus, collisions between the condensate and the impurities are visible as a circular halo which represents the line-of-sight integrated spherical shell. Figure 1 shows a typical absorption image of collisions in the free particle regime for impurity atoms with a velocity of $2\hbar k/M = 6$ cm/s, produced by counterpropagating Raman beams.

To probe for superfluidity, we produced impurity atoms at low velocities (7 mm/s) by using Raman beams which intersected at an angle of $\approx 14°$ and aligned symmetrically about the radial direction, so that the difference vector $\mathbf{q} = \mathbf{k_1} - \mathbf{k_2}$ was directed axially [12]. The trajectory of the impurity atoms was initially in the axial direction, but was soon modified by two forces: a downward gravitational acceleration along a radial direction (into the page in images and hereafter denoted as the z axis), and the radial mean-field repulsion of the $m_F = 0$ impurities from the $m_F = -1$ condensate.

The small axial velocity imparted by the Raman beams is crucial for distinguishing the products of elastic collisions from the unscattered impurities in time-of-flight imaging. Figure 2a shows a time-of-flight image of impurity scattering for the case of a low density condensate (small c). The axial velocity imparted by Raman scattering displaces the unscattered $m_F = 0$ atoms upward in the image, whereas collisions with the stationary condensate produce impurity atoms with smaller axial velocities which then appear below the unscattered atoms in the image. The acceleration of the impurities due to gravity and mean field precluded the observation of well-defined collision halos as shown in Fig. 1. In contrast, Fig. 2b shows a time-of-flight image for the case of a high density condensate (large c), for which the number of collided atoms is greatly diminished, indicating the suppression of impurity collisions due to superfluidity.

The number of collided atoms was determined by counting impurity atoms in a region of the time-of-flight image below the unscattered impurity atoms, which also contained Raman outcoupled thermal $m_F = 0$ atoms. Hence, the number of collided atoms in the counting region was obtained by subtracting the thermal background which was determined by counting a similar sized region above the unscattered impurity atoms where we expect few collision products. This number was doubled to obtain the total number of collided atoms since we expect only about half of the collision products to be in the counting region; the remainder was overlapped with the unscattered impurities because the distribution of unscattered atoms has an axial width roughly equal to the axial displacement of Raman scattered atoms in the time-of-flight images.

In studying these collisions, we discovered that the fraction of collided atoms increased with the number of outcoupled impurities (see Fig. 3). According to a perturbative treatment described below, the collision probability should be independent of the number of impurities. If the number of outcoupled atoms is increased, one would expect the collision probability to *decrease* slightly due to the reduction in the condensate density, or to *increase* slightly because the smaller condensate density implies a smaller critical velocity for dissipation. However, these effects are smaller (10%–20%) than the observed twofold increase in the collided fraction.

Rather, this large increase can be explained as a collective self-amplification of atomic scattering, akin to the recently observed super-radiant amplification of light scattering from a Bose-Einstein condensate [13]. Collisions between impurity atoms and the condensate transfer

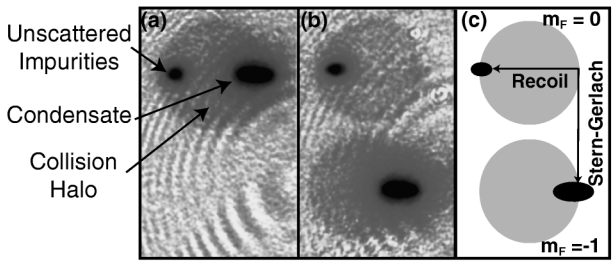

FIG. 1. Observation of s-wave halos created by elastic collisions between the condensate and impurity atoms traveling at 6 cm/s radially (right to left in images). (a) Absorption image after 50 ms of time of flight shows the velocity distribution after collisions between the condensate and the outcoupled $m_F = 0$ atoms. The collisional products are distributed over a sphere in momentum space. (b) Same as (a), but using a Stern–Gerlach-type magnetic field gradient along the condensate axis to separate the $m_F = 0$ atoms (top) from the $m_F = -1$ condensate [bottom, see (c)]. The fringes are an imaging artifact. Images are 4.5 mm × 7.2 mm. Note: the imaging axis is tilted by 45° with respect to the plane shown in (c).

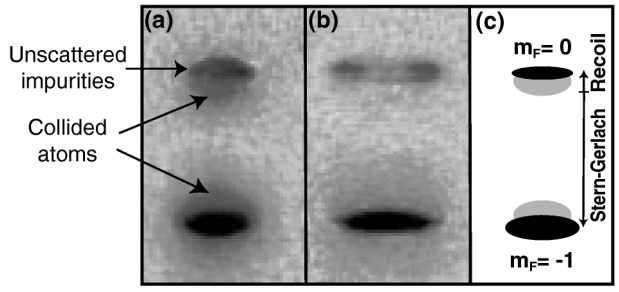

FIG. 2. Superfluid suppression of collisions. The impurity $m_F = 0$ atoms (top) traveled at 7 mm/s along the condensate axis (upward in image) and were separated from the condensate (bottom) by a magnetic field gradient applied during ballistic expansion [see (c)]. (a) Absorption image after 50 ms of time of flight shows the collisional products as indicated by the arrow. For this image, $v_g/c = 2.7$ (see text), and the collided fraction is about 20%. (b) Similar image as (a) with $v_g/c = 1.6$, where the collisions are suppressed. The outcoupled atoms (impurities) were distorted by mean-field repulsion. The images are 2.0 mm × 4.0 mm.

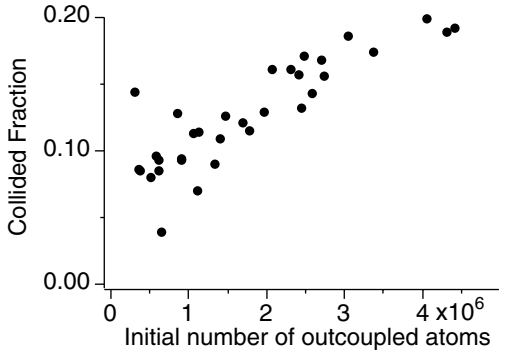

FIG. 3. Collective amplified elastic scattering in a Bose-Einstein condensate. Shown is the fraction of collided atoms vs the number of initially outcoupled atoms. For this data, $v_g/c = 4.9$ and the chemical potential was 1.8 kHz.

atoms from a macroscopically occupied initial state to final momentum states which were previously empty. The population in these final states can stimulate further scattering by bosonic enhancement and this effect increases for larger outcoupling. This collisional amplification is not directional, and is similar to the recently observed optical omnidirectional superfluorescence [14]. In contrast, the observation of four-wave mixing of atoms [15] represents the case where collisions were stimulated by a single macroscopically occupied final mode.

Figure 4 shows the decrease of collision probability as the velocity of the impurity atoms approached the speed of sound in the condensate. The collision probability was determined by averaging over many iterations of the experiment with the number of outcoupled atoms kept below 10^6 to minimize the collective enhancement. For our experimental conditions, the impurity velocity was

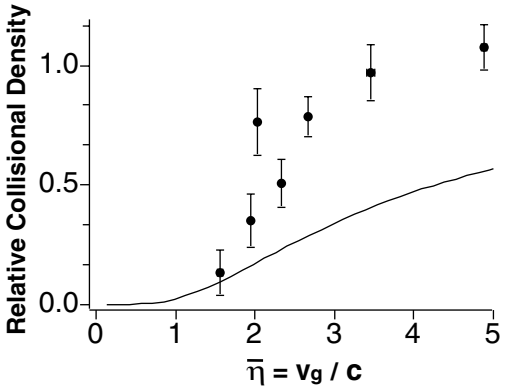

FIG. 4. Onset of superfluid suppression of collisions. Shown is the observed collisional density normalized to the predicted collisional density in the limit of high velocities C_∞ as the density of the condensate was increased (plotted from right to left). The collisional density is proportional to the collision probability of the impurities (see text). The x axis is $\overline{\eta} = v_g/c$ which is a measure of the impurity velocity over the speed of sound. The solid line is the theoretically expected collisional density calculated by a numerical integration of Eq. (1). The error bars represent the statistical uncertainty.

predominantly determined by the gravitational acceleration $g = 9.8\ \mathrm{m/s^2}$, which imparted an average velocity of $v_g = \sqrt{2gz_c}$, where z_c is the Thomas-Fermi radius of the condensate in the z direction. This downward velocity ranged from 17 mm/s for tightly confined condensates to 26 mm/s for loosely confined condensates, and was larger than the initial 7 mm/s velocity imparted by Raman scattering. Thus, the effect of superfluidity on impurity scattering depends primarily on the parameter $\overline{\eta} = v_g/c$ which is the ratio of the typical impurity velocity v_g to the speed of sound at the center of the condensate $c = \sqrt{\mu/M}$. Experimentally, $\overline{\eta}$ is determined using the radial trapping frequency and the chemical potential μ which is determined from the expansion of the condensate in the time-of-flight images [9].

Scattering of impurities from a Bose-Einstein condensate has been studied theoretically in Refs. [16,17]. The predicted cross section for collisions between an $m_F = 0$ impurity atom at momentum $\hbar\mathbf{k}$ and a $m_F = -1$ condensate of density n_0 is obtained by calculating the collision rate Γ using Fermi's golden rule:

$$\Gamma = n_0\left(\frac{\hbar a}{M}\right)^2 \int dq\, d\Omega\, q^2 S(q) \times \delta\left(\frac{\hbar\mathbf{k}\cdot\mathbf{q}}{M} - \frac{\hbar q^2}{2M} - \omega_q^B\right) = n_0\sigma(\eta)v\,,$$

Here, $S(q) = \omega_q^0/\omega_q^B$ is the static structure factor of the condensate with $\hbar\omega_q^0 = \hbar^2q^2/2M$ and $\hbar\omega_q^B = \sqrt{\hbar\omega_q^0(\hbar\omega_q^0 + 2\mu)}$ being the energies of a free particle and a Bogoliubov quasiparticle of momentum q, respectively. The collision cross section is $\sigma(\eta) = \sigma_0 F(\eta)$, where $\eta = v/c$, $v = \hbar k/M$ is the impurity velocity, and $\sigma_0 = 4\pi a_{0,-1}^2$, where $a_{0,-1} = 2.75$ nm [18] is the scattering length for s-wave collisions between the $|m_F = 0\rangle$ and $|m_F = -1\rangle$ states of sodium. For $\eta < 1$, $F(\eta) = 0$ and, for $\eta > 1$, $F(\eta) = 1 - 1/\eta^4 = \log(\eta^4)/\eta^2$.

We can approximate our experiment by considering the motion of the $m_F = 0$ atoms under the gravitational acceleration alone and ignoring the effects of the initial axial velocity and mean-field expulsion [19]. The $m_F = 0$ atoms falling through the condensate experience a collisional density $C(\eta) = \int dz\, n(x,y,z)\sigma(\eta)$, where $n(x,y,z)$ is the condensate density, and η is determined by the local condensate density and the downward impurity velocity. The collisional density relative to its value at large velocities C_∞ is given by

$$\frac{C(\overline{\eta})}{C_\infty} \approx \frac{\int d\mathbf{r}\, n_I(\mathbf{r}) \times \int dz'\, n(\mathbf{r}')\sigma_0 F(\eta)}{\int d\mathbf{r}\, n_I(\mathbf{r}) \times \int dz'\, n(\mathbf{r}')\sigma_0}\,, \qquad (1)$$

where we assume that the condensate density $n(\mathbf{r})$ is in the Thomas-Fermi limit [9] and that the initial impurity density $n_I(\mathbf{r}) \propto n(\mathbf{r})$ [20]. The solid line in Fig. 4 was determined by numerically integrating Eq. (1). To compare the collision probability for the different data points, we divided

the observed collided fraction by $C_\infty = (5/12) \times n_0 \sigma_0 z_c$. The observed decrease in the collisional density for small $\overline{\eta}$ (Fig. 4) shows the superfluid suppression of collisions. Numerical simulations ruled out the possibility that the observed decrease in collisional density could be caused solely by variations of the path length of particle trajectories due to mean-field repulsion and initial velocity.

The measured values in Fig. 4 are systematically larger by a factor of about 2 than expected theoretically. This discrepancy is also seen for impurity collisions at velocities of 6 cm/s for which superfluidity should play no role. While we cannot presently account for this systematic error in measuring absolute densities, the observation of suppression of collisions due to superfluidity is robust, since it requires only a relative comparison of collision probabilities at different $\overline{\eta}$.

The method presented here can generally be used to study ultracold collisions. In this study, we focused on collisions between atoms in different hyperfine states. By driving a Bragg transition [21] instead of a Raman transition, we have also observed collisions between atoms in the same internal state. At a velocity of 6 cm/s, we found the collision cross section to be 2.1 ± 0.3 times larger than in the Raman case, reflecting the exchange term in elastic collisions for identical particles that increases the cross section from $4\pi a^2$ to $8\pi a^2$.

Raman transitions are one way to realize output couplers for atom lasers [10,22,23]. Theoretical treatments of atom lasers have typically considered only the condensate and the outcoupled atoms in a two-mode approximation and ignored the modes accessible by collisions [24]. However, our experiment shows that, as the outcoupled atoms pass through the condensate, they collide and populate modes coupled by atomic scattering [25]; the collisions may even be enhanced by bosonic stimulation. In principle, such collisional losses can be avoided by *lowering* the density. However, an alternative route to suppressing collisions is to *increase* the density until the speed of sound is larger than the velocity of the outcoupled atoms, thus realizing a "superfluid" output coupler. Therefore, Raman transitions with small recoil or rf output couplers [22] might be most suitable for realizing atom lasers with large condensates.

In conclusion, we have studied collisions between impurity atoms and a Bose-Einstein condensate. Both the observed superfluid suppression of collisions and the collective enhancement are crucial considerations for the future development of intense atom lasers.

We are grateful to D. E. Pritchard and Y. Band for valuable discussions. This work was supported by ONR, NSF, JSEP, ARO, NASA, and David and Lucile Packard Foundation. A. P. C. acknowledges additional support from the NSF, A. G. from DAAD, and D. M. S. K. from JSEP.

*Present address: Norman Bridge Laboratory of Physics, California Institute of Technology 12-33, Pasadena, CA 91125.

[1] L. D. Landau, J. Phys. (Moscow) **5**, 71 (1941).
[2] D. R. Tilley and J. Tilley, *Superfluidity and Superconductivity* (IOP, New York, 1990), pp. 41–53.
[3] L. Meyer and F. Reif, Phys. Rev. **123**, 727 (1961); D. R. Allum, P. V. E. McClintock, A. Phillips, and R. M. Bowley, Philos. Trans. R. Soc. London A **284**, 179 (1977).
[4] J. Harms and J. P. Toennies, Phys. Rev. Lett. **83**, 344 (1999).
[5] C. Raman *et al.,* Phys. Rev. Lett. **83**, 2502 (1999).
[6] M. R. Matthews *et al.,* Phys. Rev. Lett. **83**, 2498 (1999).
[7] K. W. Madison, F. Chevy, W. Wohlleben, and J. Dalibard, Phys. Rev. Lett. **84**, 806 (2000).
[8] O. M. Marago *et al.,* Phys. Rev. Lett. **84**, 2056 (2000).
[9] W. Ketterle, D. S. Durfee, and D. M. Stamper-Kurn, in *Bose-Einstein Condensation in Atomic Gases,* Proceedings of the International School of Physics "Enrico Fermi," Course CXL, edited by M. Inguscio, S. Stringari, and C. E. Wieman (IOS Press, Amsterdam, 1999).
[10] E. W. Hagley *et al.,* Science **283**, 1706 (1999).
[11] K. Gibble, S. Chang, and R. Legere, Phys. Rev. Lett. **75**, 2666 (1995).
[12] D. M. Stamper-Kurn *et al.,* Phys. Rev. Lett. **83**, 2876 (1999).
[13] S. Inouye *et al.,* Science **285**, 571 (1999).
[14] A. I. Lvovsky, S. R. Hartmann, and F. Moshary, Phys. Rev. Lett. **82**, 4420 (1999).
[15] L. Deng *et al.,* Nature (London) **398**, 218 (1999).
[16] E. Timmermans and R. Côté, Phys. Rev. Lett. **80**, 3419 (1998).
[17] Z. Idziaszek, K. Rzazewski, and M. Wilkens, J. Phys. B **32**, L205 (1999).
[18] E. Tiesinga *et al.,* J. Res. Natl. Inst. Stand. Technol. **101**, 505 (1996); T.-L. Ho, Phys. Rev. Lett. **81**, 742 (1998).
[19] A numerical simulation showed that including these effects changes the collisional density by less than 20%.
[20] The Raman transition strength is uniform over the entire condensate since the frequency broadening due to finite pulse length (16 kHz) was larger than the broadening due to mean field (~2 kHz).
[21] J. Stenger *et al.,* Phys. Rev. Lett. **82**, 4569 (1999).
[22] M.-O. Mewes *et al.,* Phys. Rev. Lett. **78**, 582 (1997); I. Bloch, T. W. Hänsch, and T. Esslinger, Phys. Rev. Lett. **82**, 3008 (1998).
[23] B. P. Anderson and M. A. Kasevich, Science **282**, 1686 (1998).
[24] For example, R. J. Ballagh, K. Burnett, and T. F. Scott, Phys. Rev. Lett. **78**, 1607 (1997); Y. B. Band, P. S. Julienne, and M. Trippenbach, Phys. Rev. A **59**, 3823 (1999).
[25] Motivated by our results, collisions were recently included in a theoretical treatment of interaction between condensates: Y. B. Band, M. Trippenbach, J. P. Burke, Jr., and P. S. Julienne, Phys. Rev. Lett. **84**, 5462 (2000).